This article has been accepted for publication in a future issue of this journal, but has not been fully edited. Content may change prior to final publication.
Citation information: DOI: 10.1109/TSMC.2025.3612590, IEEE Transactions on Systems, Man, and Cybernetics: Systems

Recursive State Estimation for Nonlinear Cyber-Physical Systems Under Random Access Protocol: A Token Bucket Strategy

Yu-Ang Wang, Zidong Wang, Lei Zou, Fan Wang, and Hongli Dong

***Abstract*—This paper investigates the recursive state estimation problem for a class of nonlinear cyber-physical systems operating under a token bucket strategy regulated by a random access protocol. Communication between sensor nodes and the remote estimator takes place over a shared network, where only one sensor node is permitted to access the network at each time instant to prevent data collisions. The transmission sequence of sensor nodes is governed by random access protocol scheduling, which is modeled as a sequence of independent and identically distributed variables representing the selected node granted network access. To efficiently manage limited communication resources, a token bucket strategy is employed. The measurement signal from the selected node is transmitted to the estimator only if a sufficient number of tokens are available in the bucket to meet the required token consumption. The objective is to design a state estimation algorithm that minimizes the estimation error covariance by appropriately determining the estimator gain at each time step. The desired estimator gain is computed recursively by solving two Riccati-like difference equations. Finally, an illustrative example is presented to validate the effectiveness of the proposed estimation method.**

***Index Terms*—Recursive state estimation, random access protocol, token bucket strategy, nonlinear stochastic systems, cyber-physical systems.**

I. Introduction

Over the past decades, significant interest has been drawn to the study of cyber-physical systems (CPSs), which have been widely applied in various fields, including unmanned aerial navigation systems, industrial automation, environmental monitoring, sensor networks, mobile communications, and smart grids. In CPSs, signal transmission between different system components is achieved through a shared communication network, which greatly benefits from real-time sensing, control, and response to changes in the physical world, thereby enhancing autonomy, reliability, and intelligence. Generally, due to the nonlinear nature of the physical world, its dynamics must be represented by nonlinear models [6], [16], [24], [27], [43], allowing for an accurate description of the complex and varied behaviors of physical systems. Rapid technological advances have stimulated strong interest in CPSs, leading researchers to address numerous challenges in this field [2]–[4], [7], [9], [15], [28], [42], [47].

State estimation, as a fundamental problem in system science, has been extensively studied due to its wide range of applications in engineering practices, such as navigation and radar tracking systems. A substantial amount of research has been dedicated to various aspects of state estimation problems [14], [30]–[32], [44]. Among the various techniques that have been developed, Kalman filtering schemes are recognized as the most effective approach for linear systems subject to Gaussian noise, with the objective of minimizing the estimation error covariance (EEC) [5], [11]. Unfortunately, conventional Kalman filtering is not applicable to nonlinear systems. Therefore, the development of suitable estimation methods capable of effectively handling nonlinearities is of crucial importance, both from theoretical and practical perspectives. Furthermore, it should be noted that, in practice, most systems exhibit time-varying characteristics. Such variability arises primarily due to several factors, including temperature fluctuations, operating point drifts, and the aging of system components over time [13], [19], [23]. Consequently, recursive estimation for systems with both nonlinear dynamics and time-varying parameters has become a critical area of research.

An implicit assumption in many existing results on state estimation for CPSs is that all sensor nodes connected to the network can simultaneously access the communication channel for data transmission. Unfortunately, this assumption is often unrealistic in practical engineering, as multiple simultaneous accesses to a shared communication channel (with limited bandwidth) inevitably result in data collisions or conflicts. To address this issue, various communication protocols have been developed to schedule network resources based on system nodes. Some of these protocols include the try-once-discard protocol [8], [36], [39], the round-robin protocol [10], [22],

This work was supported in part by the National Natural Science Foundation of China under Grants 61933007 and 62273087, and U21A2019, the Shanghai Pujiang Program of China under Grant 22PJ1400400, the Hainan Province Science and Technology Special Fund of China under Grant ZDYF2022SHFZ105, the Royal Society of the UK, and the Alexander von Humboldt Foundation of Germany. *(Corresponding author: Zidong Wang.)*

Yu-Ang Wang and Lei Zou are with the College of Information Science and Technology, Donghua University, Shanghai 201620, China, and are also with the Engineering Research Center of Digitalized Textile and Fashion Technology, Ministry of Education, Shanghai 201620, China. (Emails: yuangwang98@163.com; zouleicup@gmail.com).

Zidong Wang is with the College of Electrical Engineering and Automation, Shandong University of Science and Technology, Qingdao 266590, China. He is also with the Department of Computer Science, Brunel University London, Uxbridge, Middlesex, UB8 3PH, United Kingdom. (Email: Zidong.Wang@brunel.ac.uk).

Fan Wang is with the School of Automation, Nanjing University of Information Science and Technology, Nanjing 210044, China. (Email: wangfan.92128@gmail.com).

Hongli Dong is with the Artificial Intelligence Energy Research Institute, Northeast Petroleum University, Daqing 163318, China, and is also with the Heilongjiang Provincial Key Laboratory of Networking and Intelligent Control, Northeast Petroleum University, Daqing 163318. (Email: shiningdhl@vip.126.com).

This article has been accepted for publication in a future issue of this journal, but has not been fully edited. Content may change prior to final publication.
Citation information: DOI: 10.1109/TSMC.2025.3612590, IEEE Transactions on Systems, Man, and Cybernetics: Systems

[35], [37], [41], and the random access protocol (RAP) [12], [33]. Among these communication protocols, RAP has been widely adopted in the industry due to its simplicity and efficacy in handling varying traffic loads. A prominent example of RAP is the carrier-sense multiple access protocol, which has been extensively utilized in wireless communication systems.

It is worth noting that, in the context of estimation problems involving protocol scheduling, the use of communication protocols introduces certain constraints. These constraints, in turn, can significantly affect overall estimation performance. Regarding networked control systems operating under various communication protocols, although the analysis and synthesis of such systems have garnered initial research interest (e.g., [17], [19], [26], [38], [45]), the issue of recursive estimation for CPSs subject to RAP has not been fully explored. This gap in the literature, along with the potential for substantial improvements in estimation performance under realistic communication constraints, has served as the primary motivation for the present research.

In CPSs, the transmission of signals over a network is always constrained by the transmission rate due to the limited availability of communication resources [46]. The token bucket strategy has been widely adopted in real-world applications for network traffic control, serving as an effective tool to address transmission constraints [18], [25], [29], [34]. This protocol allows a specific amount of data to be transmitted per attempt and is capable of handling transmissions that exceed rate limits. Conceptually, it operates like a bucket with a fixed capacity that is continuously filled with tokens over time. Token generation is paused when the bucket reaches full capacity and resumes once a token is consumed. The success of data transmissions is determined by the token generation rate and the token consumption rate.

Under the constraints of the token bucket strategy, the measurement signal is successfully transmitted over the network if a sufficient number of tokens are available in the bucket. If the number of tokens in the bucket is lower than the amount required for transmission, the transmission fails without consuming any tokens. The token bucket strategy ensures that a transmission is successful when token consumption remains below the generation rate. Even if the number of tokens consumed for transmission exceeds the number currently being generated, successful transmission can still be facilitated as long as an adequate number of tokens are present in the bucket. A dynamic model of token buckets, known as the token bucket algorithm, has been employed to describe network behavior in [21]. It should be noted that the application of token bucket techniques to CPSs, particularly in state estimation problems, remains a developing area [40], which has served as the second motivation for the present research.

As mentioned previously, the design of a state estimator for CPSs, while accounting for the impact of RAP-based token bucket strategies, is of crucial practical importance and presents several significant challenges: 1) developing techniques to minimize the upper bound of the EEC while addressing the RAP-based token bucket strategy; 2) managing measurement outputs affected by the token bucket strategy, particularly in cases of insufficient tokens, and analyzing the transient behavior of the state estimation error induced by token storage; and 3) formulating an implementation of the estimator gain matrix that incorporates information from the RAP-based token bucket strategy. The primary objective of this paper is to develop an effective strategy to comprehensively address these challenges.

Motivated by the above discussions, this paper aims to overcome the challenges associated with designing an estimator capable of handling the complexity introduced by the RAP-based token bucket strategy. This objective is achieved through the development of a recursive estimation algorithm. The main contributions of this study, which emphasize its innovation and technological advancements, are highlighted as follows.

1) For the first time, a thorough investigation is conducted into the state estimation problem for CPSs by explicitly considering the impact of the RAP-based token bucket strategy, which is an area of growing significance in both practical applications and theoretical research.
2) An innovative method is proposed for computing the upper bound of the EEC by solving two Riccati-like difference equations recursively. This approach provides a structured and effective means to address the uncertainties and dynamic variations introduced by the RAP-based token bucket strategy.
3) The estimator gain, which is essential for achieving the desired estimation accuracy, is derived through a recursive calculation method. This approach enables the gain to be dynamically adjusted, thereby significantly enhancing the reliability of the estimator.

The organization of this paper is as follows. In Section II, the foundational framework is established by introducing the system configuration and key concepts, including the system model, RAP characteristics, token bucket strategy, and state estimator design. Section III presents the theoretical contributions, where the upper bound for the EEC is derived, and the recursive computation of the estimator gain is detailed. In Section IV, the effectiveness and robustness of the proposed approach are validated through a detailed example, demonstrating its capability to address system complexities. Finally, Section V provides a summary of the main findings, highlights the contributions, and explores potential avenues for future research.

Notations: $\mathbb{R}^m$ represents the m dimensional Euclidean space and $\mathbb{R}^{m\times n}$ represents the set of all $m\times n$ real matrices. I denotes the identity matrix. 0 denotes the zero matrix. $\mathbf{1}_{m\times n}$ denotes the all-ones matrix of size $m\times n$. $\mathbf{0}_{m\times n}$ denotes the all-zeros matrix of size $m\times n$. Y^{-1} represents the inverse of the square matrix Y. M^T indicates the transpose of matrix M. Matrices without explicitly stated are supposed to have compatible dimensions for matrix operations. $\lambda_{\min}\{\mathcal{R}\}$ ($\lambda_{\max}\{\mathcal{R}\}$) stands for the minimum (maximum) eigenvalue of matrix $\mathcal{R}$. $\mathbb{P}\{\mathcal{L}\}$ denotes the occurrence probability of an event $\mathcal{L}$. $\mathbb{E}\{\varrho\}$ represents the mathematical expectation of a stochastic variable ϱ.

This article has been accepted for publication in a future issue of this journal, but has not been fully edited. Content may change prior to final publication.
Citation information: DOI: 10.1109/TSMC.2025.3612590, IEEE Transactions on Systems, Man, and Cybernetics: Systems

II. Problem Formulation

A. System Model

The plant dynamics and corresponding measurements are characterized as follows:

$$\begin{cases} x_{s+1} = f(x_s) + A_s x_s + B_s \omega_s \\ y_s = C_s x_s + D_s \nu_s \end{cases} \tag{1}$$

where $x_s \in \mathbb{R}^{n_x}$ represents the state variable, and $y_s \in \mathbb{R}^{n_y}$ denotes the measurement output. $\nu_s \in \mathbb{R}^{n_\nu}$ and $\omega_s \in \mathbb{R}^{n_\omega}$ are the measurement noise and the process noise, respectively. These noises are modeled as mutually uncorrelated zero-mean sequences with covariance properties $\mathbb{E}\{\omega_s \omega_s^T\} = W_s$ and $\mathbb{E}\{\nu_s \nu_s^T\} = V_s$. The time-varying matrices A_s, B_s, C_s and D_s have appropriate dimensions. The initial condition of x_s has a known mean value and is assumed to be independent of the noises. The nonlinear function $f(\cdot) : \mathbb{R}^{n_x} \to \mathbb{R}^{n_x}$ adheres to the following constraints:

$$f(0) = 0, \quad \|f(\pi_1) - f(\pi_2)\| \le \alpha \|\pi_1 - \pi_2\| \tag{2}$$

where $\pi_1, \pi_2 \in \mathbb{R}^{n_x}$ are arbitrary vectors, and α is a known positive scalar.

B. Random-Access-Protocol-Based Token Bucket Strategy

Let us now discuss the signal transmission within the communication network. To facilitate analysis, we assume that sensors of the system are grouped into n sensor nodes based on their spatial distribution. Under this assumption, the measurement output prior to transmission can be expressed as:

$$y_s \triangleq \begin{bmatrix} y_{1,s} & y_{2,s} & \cdots & y_{n,s} \end{bmatrix}^T$$

where $y_{i,s}$ ($i \in \{1, 2, \ldots, n\}$) represents the measurement of the i-th sensor node before it is transmitted.

To avoid data collisions during transmission, only one sensor node is allowed to access the communication network at any given transmission instant. This network access constraint necessitates the use of scheduling protocols to determine the transmission order of sensor nodes. In this paper, RAP is adopted for scheduling transmissions. Let κ_s ($\kappa_s \in \{1, 2, \ldots, n\}$) denote the selected node to transmit data at time instant s. As shown in [33], $\{\kappa_s\}_{s \ge 0}$ can be modeled as a sequence of mutually independent random variables. The probability of selecting node i ($i \in \{1, 2, \ldots, n\}$) for transmission at time instant s is given by:

$$\text{Prob}\{\kappa_s = i\} = b_i \tag{3}$$

where $1 > b_i > 0$ is the probability that node i is chosen to transmit data via the communication network and satisfies $\sum_{i=1}^{n} b_i = 1$.

Denoting the measurement output after transmission through the network as:

$$\vec{y}_s \triangleq \begin{bmatrix} \vec{y}_{1,s} & \vec{y}_{2,s} & \cdots & \vec{y}_{n,s} \end{bmatrix}^T, \tag{4}$$

the updating rule of $\vec{y}_{i,s}$ under RAP scheduling is set as follows:

$$\vec{y}_{i,s} = \begin{cases} y_{i,s}, & \text{if} \quad i = \kappa_s, \ s \ge 0 \\ 0, & \text{otherwise.} \end{cases} \tag{5}$$

According to the updating rule (5), it can be seen that

$$\begin{cases} \vec{y}_s = \Psi_s y_s, & \text{if} \quad s \ge 0 \\ \vec{y}_s = 0, & \text{otherwise} \end{cases} \tag{6}$$

where $\Psi_s \triangleq \text{diag}\{\delta(\kappa_s - 1)I, \delta(\kappa_s - 2)I, \ldots, \delta(\kappa_s - n)I\}$ and $\delta(\cdot) \in \{0, 1\}$ is the Kronecker delta function.

Without loss of generality, consider the case where the i-th element $\vec{y}_{i,s}$ lies within the interval $[-L_i, L_i]$, where $L_i \in \mathbb{R}$ is a known positive scalar determined by the sensor characteristics. To quantize $\vec{y}_{i,s}$, a quantization accuracy $\theta_i \in \mathbb{R}$, representing the number of intervals, is chosen. Based on this accuracy, the range of $\vec{y}_{i,s}$ is uniformly divided into θ_i subintervals, which are defined as follows:

$$\begin{cases} Q_{1,i}: & -L_i \le \vec{y}_{i,s} < -L_i + \dfrac{2L_i}{\theta_i} \\ Q_{2,i}: & -L_i + \dfrac{2L_i}{\theta_i} \le \vec{y}_{i,s} < -L_i + \dfrac{4L_i}{\theta_i} \\ \quad \vdots & \\ Q_{\theta_i,i}: & L_i - \dfrac{2L_i}{\theta_i} \le \vec{y}_{i,s} < L_i. \end{cases} \tag{7}$$

For simplicity, define

$$\mathcal{T}_i \triangleq \frac{2L_i}{\theta_i}, \tag{8}$$

then the number of bits assigned to $\vec{y}_{i,s}$ is given by:

$$R_i = \lceil \log_2 \mathcal{T}_i \rceil \tag{9}$$

where $\lceil \log_2 \mathcal{T}_i \rceil$ represents the smallest integer greater than or equal to $\log_2 \mathcal{T}_i$, corresponding to the minimum number of bits required to represent $\mathcal{T}_i$ in binary form.

To regulate the transmission rate and ensure efficient utilization of available bandwidth, the token bucket strategy is employed for transmitting measurement outputs. At any time step s, let the bucket level be denoted as $z_s \in \{0, 1, 2, \cdots, S\}$, where S is the bucket's maximum token capacity ($S > \varepsilon$), and ε is the constant token generation rate per time step. Given the initial condition $z_0 \le S$, the dynamics of the bucket level can be expressed as:

$$z_{s+1} = \min\{z_s + \varepsilon, S\} - \mu_s \varphi_s \tag{10}$$

where φ_s represents the number of tokens consumed at time s, and μ_s is an indicator function defined as:

$$\mu_s \triangleq \begin{cases} 1, & \min\{z_s + \varepsilon, S\} - \varphi_s \ge 0, \\ 0, & \text{otherwise.} \end{cases} \tag{11}$$

The level of tokens consumed, φ_s, follows a probabilistic distribution influenced by the RAP. At each time step, the random selection of sensor nodes for data transmission introduces fluctuations in the token consumption rate, which is governed by the number of bits assigned to each node. Simultaneously, the probability of token consumption is determined by the probability of selecting the i-th node. Consequently, by utilizing (3), (9) and (10), the probability distribution of φ_s is given by:

$$\text{Prob}\{\varphi_s = R_i\} = b_i \tag{12}$$

This article has been accepted for publication in a future issue of this journal, but has not been fully edited. Content may change prior to final publication.
Citation information: DOI: 10.1109/TSMC.2025.3612590, IEEE Transactions on Systems, Man, and Cybernetics: Systems

where R_i is the number of bits required for the i-th measurement signal, and b_i, introduced in (3), is the probability of selecting the corresponding sensor node for transmission.

The token bucket operates as a repository where tokens are generated at a constant rate ε per time step. Once the bucket reaches its maximum capacity S, token generation is halted until tokens are consumed. At each time step, the ability to transmit measurement signals depends on the availability of sufficient tokens. If enough tokens are present, the signal is transmitted, consuming a specified number of tokens. Otherwise, the signal is not transmitted, and no tokens are consumed.

In this paper, priority is given to token generation over consumption at each time instant s. This implies that tokens are first generated, after which a decision is made regarding their consumption for data transmission. By allowing token consumption to potentially exceed token generation in a single step, this approach provides the flexibility required to adapt to variable data transmission demands. Such adaptability is essential for optimizing network resources and maintaining efficient data flow.

Following the previous discussions, the measurement signal can be expressed as follows:

$$\tilde{y}_s = \mu_s \vec{y}_s. \tag{13}$$

Remark 1: RAP is widely utilized as a scheduling protocol to address network access constraints in wireless communications. By incorporating probabilistic information during communication channel allocation, RAP facilitates efficient scheduling in unreliable environments [8]. This protocol was first introduced in [33] and [8], where continuous-time and discrete-time systems were studied, respectively. A notable example of RAP scheduling is the carrier-sense multiple access protocol, which has been successfully implemented in the industry to effectively mitigate the issue of limited communication channel capacity [1], [48].

Remark 2: The probability distribution of token consumption levels, as described in (12), has been carefully designed and is directly influenced by the RAP scheduling mechanism. The random selection of sensor nodes for data transmission at each time step leads to fluctuations in token consumption rates, which depend on the number of bits allocated to each node. This probabilistic approach effectively models the adaptive nature of data transmission in CPS environments, capturing the dynamic interplay between scheduling protocols and communication constraints. Moreover, it underscores the inherent challenges associated with achieving efficient and reliable communication in systems with limited network resources.

C. State Estimator

For CPS described by (1) with measurement outputs characterized by (13), a state estimator with the following structure is employed:

$$\begin{cases} \hat{x}_{s+1|s} = A_s \hat{x}_{s|s} + f(\hat{x}_{s|s}) \\ \hat{x}_{s+1|s+1} = \hat{x}_{s+1|s} + K_{s+1}\Big(\tilde{y}_{s+1} \\ \qquad\qquad - \vec{\mu}_{s+1}\Psi_{s+1}C_{s+1}\hat{x}_{s+1|s}\Big) \end{cases} \tag{14}$$

where $\hat{x}_{s+1|s} \in \mathbb{R}^{n_x}$ represents the one-step prediction of x_{s+1}, and $\hat{x}_{s+1|s+1} \in \mathbb{R}^{n_x}$ represents the state estimate of x_{s+1}. The matrix $K_{s+1} \in \mathbb{R}^{n_x \times n}$ is the estimator gain to be designed, and

$$\vec{\mu}_{s+1} \triangleq \mathbb{E}\{\mu_{s+1}\},$$

whose specific form will be introduced later.

The one-step prediction error and estimation error are defined as $e_{s+1|s} \triangleq x_{s+1} - \hat{x}_{s+1|s}$ and $e_{s+1|s+1} \triangleq x_{s+1} - \hat{x}_{s+1|s+1}$, respectively. Their associated covariances are denoted as $P_{s+1|s} \triangleq \mathbb{E}\{e_{s+1|s}e_{s+1|s}^T\}$ and $P_{s+1|s+1} \triangleq \mathbb{E}\{e_{s+1|s+1}e_{s+1|s+1}^T\}$.

Based on (1), (13) and (14), the error dynamics are expressed as:

$$\begin{cases} e_{s+1|s} = f(e_{s|s}) + A_s e_{s|s} + B_s \omega_s \\ e_{s+1|s+1} = (I - \vec{\mu}_{s+1}K_{s+1}\Psi_{s+1}C_{s+1})\, e_{s+1|s} \\ \qquad\qquad - K_{s+1}\left(\mu_{s+1} - \vec{\mu}_{s+1}\right) C_{s+1}\Psi_{s+1}x_{s+1} \\ \qquad\qquad - K_{s+1}\mu_{s+1}\Psi_{s+1}D_{s+1}\nu_{s+1} \end{cases} \tag{15}$$

where

$$f(e_{s|s}) \triangleq f(x_s) - f(\hat{x}_{s|s}).$$

The aim of this paper is to design a state estimator of the form (14) for the system described in (1), achieving the following objectives:

1) Derive the upper bounds $\bar{\mathcal{M}}_{s+1|s}$ and $\bar{\mathcal{M}}_{s+1|s+1}$ for the prediction and estimation error covariances, ensuring:
$$P_{s+1|s} \le \bar{\mathcal{M}}_{s+1|s}, \quad P_{s+1|s+1} \le \bar{\mathcal{M}}_{s+1|s+1}.$$
2) Design the estimator gain K_{s+1} through recursive calculation to minimize the upper bound $\bar{\mathcal{M}}_{s+1|s+1}$.

III. Main Results

An upper bound on the EEC is first calculated in this section. Subsequently, the estimator gain is derived by minimizing the upper bound. The following lemmas establish the theoretical foundation for the key results presented in this section.

Lemma 1: [20] For a positive scalar β and any given vectors $\hbar$ and ϱ, the following inequality holds:

$$\hbar\varrho^T + \varrho\hbar^T \le \beta\hbar\hbar^T + \beta^{-1}\varrho\varrho^T. \tag{16}$$

Lemma 2: Let $\{z_s\}_{s\ge 0}$ denote the token bucket level whose probability distribution is characterized by (10). Define the probability distribution vector at time instant s as $\chi_s \triangleq \begin{bmatrix}\text{Prob}\{z_s=0\} & \text{Prob}\{z_s=1\} & \cdots & \text{Prob}\{z_s=S\}\end{bmatrix}^T$. The recursion for χ_s is given by:

$$\chi_{s+1} = \left(\begin{bmatrix}\mathcal{W}_1 & \mathcal{W}_2 & \mathcal{W}_3 \\ \mathcal{W}_4 & \mathcal{W}_5 & \mathcal{W}_6 \\ \mathcal{W}_7 & \mathcal{W}_8 & \mathcal{W}_9\end{bmatrix} + \Omega\Xi\right)\chi_s \tag{17}$$

whose initial condition is given by:

$$\chi_0 = \Big[\underbrace{0 \quad \cdots \quad 0}_{z_0} \quad 1 \quad \underbrace{0 \quad \cdots \quad 0}_{S-z_0}\Big]^T$$

This article has been accepted for publication in a future issue of this journal, but has not been fully edited. Content may change prior to final publication.
Citation information: DOI: 10.1109/TSMC.2025.3612590, IEEE Transactions on Systems, Man, and Cybernetics: Systems

where

$$\mathcal{W}_2 \triangleq \begin{bmatrix} b_{\varepsilon+1} & b_{\varepsilon+2} & \dots & b_{S-1} \\ b_{\varepsilon} & b_{\varepsilon+1} & \dots & b_{S-2} \\ \vdots & \vdots & \ddots & \vdots \\ b_1 & b_2 & \dots & b_{S-\varepsilon-1} \end{bmatrix},$$

$$\mathcal{W}_1 \triangleq \begin{bmatrix} b_{\varepsilon} \\ b_{\varepsilon-1} \\ \vdots \\ b_0 \end{bmatrix}, \quad \mathcal{W}_5 \triangleq \begin{bmatrix} b_0 & b_1 & \dots & b_{S-\varepsilon-2} \\ 0 & b_0 & \dots & b_{S-\varepsilon-3} \\ \vdots & \vdots & \ddots & \vdots \\ 0 & 0 & \dots & b_0 \end{bmatrix},$$

$$\mathcal{W}_3 \triangleq \begin{bmatrix} b_S & b_{S-1} & \dots & b_{S-\varepsilon} \end{bmatrix}^T \otimes \mathbf{1}_{1\times(\varepsilon+1)},$$

$$\mathcal{W}_6 \triangleq \begin{bmatrix} b_{S-\varepsilon-1} & b_{S-\varepsilon-2} & \dots & b_1 \end{bmatrix}^T \otimes \mathbf{1}_{1\times(\varepsilon+1)},$$

$$\mathcal{W}_4 \triangleq \mathbf{0}_{(S-\varepsilon-1)\times 1}, \quad \mathcal{W}_8 \triangleq \mathbf{0}_{1\times(S-\varepsilon-1)},$$

$$\mathcal{W}_7 \triangleq 0, \quad \mathcal{W}_9 \triangleq b_0 \otimes \mathbf{1}_{1\times(\varepsilon+1)},$$

$$\Omega \triangleq \operatorname{diag}\left\{\sum_{g=1}^{S} b_g, \sum_{g=2}^{S} b_g, \dots, b_S, 0\right\},$$

$$\Xi \triangleq \begin{bmatrix} 0_{\varepsilon\times(S-\varepsilon+1)} & 0_{\varepsilon\times\varepsilon} \\ I & 0_{(S-\varepsilon+1)\times\varepsilon} \end{bmatrix}.$$

Proof: According to (10), the probability of z_{s+1} satisfies:

$$\begin{aligned} &\operatorname{Prob}\{z_{s+1}=m\} \\ &=\sum_{\tau=1}^{S-m}\operatorname{Prob}\{z_s=m-\varepsilon,\varphi_s=m+\tau\} \\ &\quad+\sum_{\tau=0}^{S-\varepsilon-1}\operatorname{Prob}\{z_s=\tau,\varphi_s=\tau+\varepsilon-m\} \\ &\quad+\sum_{\tau=0}^{\varepsilon}\operatorname{Prob}\{z_s=S-\varepsilon+\tau,\varphi_s=S-m\}. \end{aligned} \tag{18}$$

Drawing upon the fact that, at time instant s, z_s and φ_s are independent of each other, (18) can be rewritten as:

$$\begin{aligned} &\operatorname{Prob}\{z_{s+1}=m\} \\ &=\sum_{\tau=1}^{S-m} b_{m+\tau}\operatorname{Prob}\{z_s=m-\varepsilon\}+\sum_{\tau=0}^{S-\varepsilon-1} b_{\tau+\varepsilon-m} \\ &\quad\times\operatorname{Prob}\{z_s=\tau\}+\sum_{\tau=0}^{\varepsilon} b_{S-m}\operatorname{Prob}\{z_s=S-\varepsilon+\tau\} \\ &=\sum_{\tau=m+1}^{S} b_{\tau}\operatorname{Prob}\{z_s=m-\varepsilon\}+\sum_{\tau=0}^{S-\varepsilon-1} b_{\tau+\varepsilon-m} \\ &\quad\times\operatorname{Prob}\{z_s=\tau\}+b_{S-m}\sum_{\tau=S-\varepsilon}^{\varepsilon}\operatorname{Prob}\{z_s=\tau\}. \end{aligned} \tag{19}$$

By expanding χ_{s+1} with (19), (17) is obtained, thereby completing the proof. ∎

With the recursion of the probability distribution in Lemma 2, $\vec{\mu}_{s+1}$ can be obtained as:

$$\vec{\mu}_{s+1} = 1 - \rho\chi_{s+1} \tag{20}$$

where

$$\rho \triangleq \begin{bmatrix} \sum_{g=\varepsilon+1}^{S} b_g & \sum_{g=\varepsilon+2}^{S} b_g & \cdots & b_S & 0_{1\times(\varepsilon+1)} \end{bmatrix}. \tag{21}$$

Remark 3: The first term on the right-hand side of (19) accounts for the scenario in which a transmission failure occurs, indicating that no data has been successfully transmitted due to insufficient tokens or other network constraints. The second term represents the case where transmission is successful under the condition $z_s + \varepsilon < S$, implying that the token bucket still has the capacity to accommodate additional tokens without reaching its maximum limit. Lastly, the third term describes a successful transmission scenario in which the token bucket has already reached its maximum allowable capacity S, ensuring that no further accumulation of tokens occurs before the transmission takes place.

In the following theorem, upper bounds for the error covariances are established.

Theorem 1: Let α, β_1, β_2, and $\tilde{\beta}$ be given positive scalars. Assume that there are two sequences of matrices, denoted by $\{\bar{\mathcal{M}}_{s+1|s}\}_{s\geq 0}$ and $\{\bar{\mathcal{M}}_{s+1|s+1}\}_{s\geq 0}$ (with the initial condition $\bar{\mathcal{M}}_{0|0} = P_{0|0}$) which satisfy the following difference equations:

$$\begin{aligned} &\bar{\mathcal{M}}_{s+1|s} \\ &=(1+\beta_1)\,A_s\bar{\mathcal{M}}_{s|s}A_s^T+B_sW_sB_s^T \\ &\quad+\alpha^2\left(1+\beta_1^{-1}\right)\operatorname{tr}\left\{\bar{\mathcal{M}}_{s|s}\right\}I, \end{aligned} \tag{22}$$

$$\begin{aligned} &\bar{\mathcal{M}}_{s+1|s+1} \\ &=(1+\beta_2)\sum_{i=1}^{n} b_i\left(I-\vec{\mu}_{s+1}K_{s+1}\Psi_iC_{s+1}\right)\bar{\mathcal{M}}_{s+1|s} \\ &\quad\times\left(I-\vec{\mu}_{s+1}K_{s+1}\Psi_iC_{s+1}\right)^T+\left(1+\tilde{\beta}\right)\left(1+\beta_2^{-1}\right) \\ &\quad\times\left(\vec{\mu}_{s+1}-\vec{\mu}_{s+1}^2\right)\sum_{i=1}^{n} b_iK_{s+1}\Psi_iC_{s+1}\bar{\mathcal{M}}_{s+1|s}C_{s+1}^T \\ &\quad\times\Psi_iK_{s+1}^T+\left(1+\tilde{\beta}^{-1}\right)\left(1+\beta_2^{-1}\right)\left(\vec{\mu}_{s+1}-\vec{\mu}_{s+1}^2\right) \\ &\quad\times\sum_{i=1}^{n} b_iK_{s+1}\Psi_iC_{s+1}\hat{x}_{s+1|s}\hat{x}_{s+1|s}^TC_{s+1}^T\Psi_iK_{s+1}^T \\ &\quad+\vec{\mu}_{s+1}\sum_{i=1}^{n} b_iK_{s+1}\Psi_iD_{s+1}V_{s+1}D_{s+1}^T\Psi_iK_{s+1}^T. \end{aligned} \tag{23}$$

Then, the solution of (23) is an upper bound of $P_{s+1|s+1}$.

Proof: This theorem can be proved by the mathematical induction. To begin, it is evident that the initial condition $P_{0|0} \leq \bar{\mathcal{M}}_{0|0}$ holds. Now, assume that $P_{s|s} \leq \bar{\mathcal{M}}_{s|s}$ is satisfied, the next step is to verify that $P_{s+1|s+1} \leq \bar{\mathcal{M}}_{s+1|s+1}$ also holds.

By using the definition of the prediction error covariance $P_{s+1|s}$ and the error dynamics in (15), we obtain

$$\begin{aligned} &P_{s+1|s} \\ &=\mathbb{E}\left\{\left(f(e_{s|s})+A_se_{s|s}+B_s\omega_s\right)\right. \\ &\quad\left.\times\left(f(e_{s|s})+A_se_{s|s}+B_s\omega_s\right)^T\right\} \\ &=\mathbb{E}\left\{A_se_{s|s}e_{s|s}^TA_s^T\right\}+\mathbb{E}\left\{f(e_{s|s})f^T(e_{s|s})\right\} \\ &\quad+\mathbb{E}\left\{A_se_{s|s}f^T(e_{s|s})+f(e_{s|s})e_{s|s}^TA_s^T\right\} \\ &\quad+\mathbb{E}\left\{B_s\omega_s\omega_s^TB_s^T\right\}. \end{aligned} \tag{24}$$

This article has been accepted for publication in a future issue of this journal, but has not been fully edited. Content may change prior to final publication.
Citation information: DOI: 10.1109/TSMC.2025.3612590, IEEE Transactions on Systems, Man, and Cybernetics: Systems

With the aid of (2), one has that

$$\begin{aligned}&\mathbb{E}\left\{f(e_{s|s})f^T(e_{s|s})\right\}\leq\mathbb{E}\left\{f^T(e_{s|s})f(e_{s|s})I\right\}\\&\leq\alpha^2\mathbb{E}\left\{e_{s|s}^Te_{s|s}I\right\}\leq\alpha^2\mathrm{tr}\left\{P_{s|s}\right\}I.\end{aligned}\tag{25}$$

Furthermore, based on Lemma 1, we obtain

$$\begin{aligned}&\mathbb{E}\left\{A_se_{s|s}f^T(e_{s|s})+f(e_{s|s})e_{s|s}^TA_s^T\right\}\\&\leq\beta_1\mathbb{E}\left\{A_se_{s|s}e_{s|s}^TA_s^T\right\}+\beta_1^{-1}\mathbb{E}\Big\{f(e_{s|s})f^T(e_{s|s})\Big\}.\end{aligned}\tag{26}$$

Substituting (25) and (26) into (24), we derive

$$\begin{aligned}P_{s+1|s}\leq&(1+\beta_1)A_sP_{s|s}A_s^T+B_sW_sB_s^T\\&+\alpha^2(1+\beta_1^{-1})\mathrm{tr}\left\{P_{s|s}\right\}I\end{aligned}\tag{27}$$

which implies $P_{s+1|s}\leq\bar{\mathcal{M}}_{s+1|s}$.

Next, it is necessary to demonstrate that $P_{s+1|s+1}\leq\bar{\mathcal{M}}_{s+1|s+1}$ holds. Similarly, it follows from the definition of $P_{s+1|s+1}$ and (15) that

$$\begin{aligned}&P_{s+1|s+1}\\=&\mathbb{E}\Big\{\left(I-K_{s+1}\vec{\mu}_{s+1}\Psi_{s+1}C_{s+1}\right)e_{s+1|s}e_{s+1|s}^T\\&\times\left(I-K_{s+1}\vec{\mu}_{s+1}\Psi_{s+1}C_{s+1}\right)^T\Big\}\\&+\mathbb{E}\Big\{K_{s+1}\Big(\mu_{s+1}-\vec{\mu}_{s+1}\Big)\Psi_{s+1}C_{s+1}x_{s+1}\\&\times x_{s+1}^TC_{s+1}^T\Psi_{s+1}^T\Big(\mu_{s+1}-\vec{\mu}_{s+1}\Big)^TK_{s+1}^T\Big\}\\&+\mathbb{E}\Big\{K_{s+1}\mu_{s+1}\Psi_{s+1}D_{s+1}\nu_{s+1}\nu_{s+1}^TD_{s+1}^T\\&\times\Psi_{s+1}^T\mu_{s+1}^TK_{s+1}^T\Big\}-\mathfrak{T}_{s+1}-\mathfrak{T}_{s+1}^T\end{aligned}\tag{28}$$

where $\mathfrak{T}_{s+1}$ is defined as:

$$\begin{aligned}\mathfrak{T}_{s+1}\triangleq&\mathbb{E}\Big\{\left(I-K_{s+1}\vec{\mu}_{s+1}\Psi_{s+1}C_{s+1}\right)e_{s+1|s}\\&\times x_{s+1}^TC_{s+1}^T\Psi_{s+1}^T\Big(\mu_{s+1}-\vec{\mu}_{s+1}\Big)^TK_{s+1}^T\Big\}.\end{aligned}$$

Based on Lemma 1, we have

$$\begin{aligned}&-\mathfrak{T}_{s+1}-\mathfrak{T}_{s+1}^T\\\leq&\beta_2\mathbb{E}\Big\{\left(I-K_{s+1}\vec{\mu}_{s+1}\Psi_{s+1}C_{s+1}\right)e_{s+1|s}e_{s+1|s}^T\\&\times\left(I-K_{s+1}\vec{\mu}_{s+1}\Psi_{s+1}C_{s+1}\right)^T\Big\}\\&+\beta_2^{-1}\mathbb{E}\Big\{K_{s+1}\Big(\mu_{s+1}-\vec{\mu}_{s+1}\Big)\Psi_{s+1}C_{s+1}x_{s+1}\\&\times x_{s+1}^TC_{s+1}^T\Psi_{s+1}^T\Big(\mu_{s+1}-\vec{\mu}_{s+1}\Big)K_{s+1}^T\Big\}.\end{aligned}$$

Consequently, (28) can be rewritten as:

$$\begin{aligned}&P_{s+1|s+1}\\=&(1+\beta_2)\mathbb{E}\Big\{\left(I-K_{s+1}\vec{\mu}_{s+1}\Psi_{s+1}C_{s+1}\right)e_{s+1|s}\\&\times e_{s+1|s}^T\left(I-K_{s+1}\vec{\mu}_{s+1}\Psi_{s+1}C_{s+1}\right)^T\Big\}\\&+(1+\beta_2^{-1})\mathbb{E}\Big\{K_{s+1}\Big(\mu_{s+1}-\vec{\mu}_{s+1}\Big)\Psi_{s+1}C_{s+1}\\&\times x_{s+1}x_{s+1}^TC_{s+1}^T\Psi_{s+1}^T\Big(\mu_{s+1}-\vec{\mu}_{s+1}\Big)K_{s+1}^T\Big\}\\&+\mathbb{E}\Big\{K_{s+1}\mu_{s+1}\Psi_{s+1}D_{s+1}\nu_{s+1}\nu_{s+1}^T\\&\times D_{s+1}^T\Psi_{s+1}^T\mu_{s+1}K_{s+1}^T\Big\}\end{aligned}\tag{29}$$

and, furthermore, it is straightforward to observe that

$$\begin{aligned}&\mathbb{E}\left\{x_{s+1}x_{s+1}^T\right\}\\=&\mathbb{E}\left\{\left(e_{s+1|s}+\hat{x}_{s+1|s}\right)\left(e_{s+1|s}+\hat{x}_{s+1|s}^T\right)\right\}\\\leq&\left(1+\tilde{\beta}\right)P_{s+1|s}+\left(1+\tilde{\beta}^{-1}\right)\hat{x}_{s+1|s}\hat{x}_{s+1|s}^T.\end{aligned}\tag{30}$$

One the other hand, we from the definition of Ψ_{s+1} that

$$\Psi_{s+1}=\sum_{i=1}^n\delta(\kappa_{s+1}-i)\Psi_i.\tag{31}$$

Since

$$\delta(\kappa_{s+1}-i)\delta(\kappa_{s+1}-j)=\begin{cases}\delta(\kappa_{s+1}-i),&\text{if}\quad i=j\\0,&\text{otherwise.}\end{cases}\tag{32}$$

and

$$\mathbb{E}\left\{\delta(\kappa_{s+1}-i)\right\}=\sum_{j=1}^nb_j\delta(j-i)=b_i,\tag{33}$$

we conclude that

$$\begin{aligned}&\mathbb{E}\Big\{\left(I-K_{s+1}\vec{\mu}_{s+1}\Psi_{s+1}C_{s+1}\right)e_{s+1|s}\\&\times e_{s+1|s}^T\left(I-K_{s+1}\vec{\mu}_{s+1}\Psi_{s+1}C_{s+1}\right)^T\Big\}\\=&\mathbb{E}\Bigg\{\left(I-K_{s+1}\vec{\mu}_{s+1}\sum_{i=1}^n\delta(\kappa_{s+1}-i)\Psi_iC_{s+1}\right)e_{s+1|s}\\&\times e_{s+1|s}^T\left(I-K_{s+1}\vec{\mu}_{s+1}\sum_{i=1}^n\delta(\kappa_{s+1}-i)\Psi_iC_{s+1}\right)^T\Bigg\}\\=&P_{s+1|s}-\mathbb{E}\Bigg\{\sum_{i=1}^n\delta(\kappa_{s+1}-i)K_{s+1}\vec{\mu}_{s+1}\Psi_i\\&\times C_{s+1}e_{s+1|s}e_{s+1|s}^T\Bigg\}-\mathbb{E}\Bigg\{\sum_{i=1}^n\delta(\kappa_{s+1}-i)e_{s+1|s}\\&\times e_{s+1|s}^TC_{s+1}^T\Psi_i\vec{\mu}_{s+1}K_{s+1}^T\Bigg\}+\mathbb{E}\Bigg\{\sum_{i=1}^n\delta(\kappa_{s+1}-i)\\&K_{s+1}\vec{\mu}_{s+1}\Psi_iC_{s+1}e_{s+1|s}e_{s+1|s}^TC_{s+1}^T\Psi_i\vec{\mu}_{s+1}K_{s+1}^T\Bigg\}\\=&\sum_{i=1}^nb_i\left(I-K_{s+1}\vec{\mu}_{s+1}\Psi_iC_{s+1}\right)P_{s+1|s}\\&\times\left(I-K_{s+1}\vec{\mu}_{s+1}\Psi_iC_{s+1}\right)^T.\end{aligned}\tag{34}$$

Similarly, we also obtain

$$\begin{aligned}&\mathbb{E}\Bigg\{K_{s+1}\Big(\mu_{s+1}-\vec{\mu}_{s+1}\Big)\Psi_{s+1}C_{s+1}\\&\times\hat{x}_{s+1|s}\hat{x}_{s+1|s}^TC_{s+1}^T\Psi_{s+1}^T\Big(\mu_{s+1}-\vec{\mu}_{s+1}\Big)K_{s+1}^T\Bigg\}\\=&\sum_{i=1}^nb_i\Big(\vec{\mu}_{s+1}-\vec{\mu}_{s+1}^2\Big)K_{s+1}\Psi_iC_{s+1}\\&\times\hat{x}_{s+1|s}\hat{x}_{s+1|s}^TC_{s+1}^T\Psi_iK_{s+1}^T,\end{aligned}\tag{35}$$

This article has been accepted for publication in a future issue of this journal, but has not been fully edited. Content may change prior to final publication.
Citation information: DOI: 10.1109/TSMC.2025.3612590, IEEE Transactions on Systems, Man, and Cybernetics: Systems

$$
\begin{aligned}
&\mathbb{E}\Big\{K_{s+1}\Big(\mu_{s+1}-\vec{\mu}_{s+1}\Big)\Psi_{s+1}C_{s+1}\\
&\quad\times P_{s+1|s}C_{s+1}^T\Psi_{s+1}^T\Big(\mu_{s+1}-\vec{\mu}_{s+1}\Big)K_{s+1}^T\Big\}\\
=&\sum_{i=1}^{n}b_i\Big(\vec{\mu}_{s+1}-\vec{\mu}_{s+1}^2\Big)K_{s+1}\Psi_iC_{s+1}\\
&\quad\times P_{s+1|s}C_{s+1}^T\Psi_iK_{s+1}^T, \qquad (36)\\
&\mathbb{E}\Big\{K_{s+1}\mu_{s+1}\Psi_{s+1}D_{s+1}\nu_{s+1}\nu_{s+1}^TD_{s+1}^T\\
&\quad\times\Psi_{s+1}^T\mu_{s+1}K_{s+1}^T\Big\}\\
=&\sum_{i=1}^{n}b_i\vec{\mu}_{s+1}K_{s+1}\Psi_iD_{s+1}V_{s+1}D_{s+1}^T\Psi_iK_{s+1}^T. \qquad (37)
\end{aligned}
$$

As a result of the above derivations, we obtain

$$
\begin{aligned}
&P_{s+1|s+1}\\
\le&(1+\beta_2)\sum_{i=1}^{n}b_i\left(I-K_{s+1}\vec{\mu}_{s+1}\Psi_iC_{s+1}\right)P_{s+1|s}\\
&\times\left(I-K_{s+1}\vec{\mu}_{s+1}\Psi_iC_{s+1}\right)^T\\
&+\Big(1+\tilde{\beta}\Big)\left(1+\beta_2^{-1}\right)\Big(\vec{\mu}_{s+1}-\vec{\mu}_{s+1}^2\Big)\\
&\times\sum_{i=1}^{n}b_iK_{s+1}\Psi_iC_{s+1}P_{s+1|s}C_{s+1}^T\Psi_iK_{s+1}^T\\
&+\Big(1+\tilde{\beta}^{-1}\Big)\left(1+\beta_2^{-1}\right)\Big(\vec{\mu}_{s+1}-\vec{\mu}_{s+1}^2\Big)\\
&\times\sum_{i=1}^{n}b_iK_{s+1}\Psi_iC_{s+1}\hat{x}_{s+1|s}\hat{x}_{s+1|s}^TC_{s+1}^T\Psi_iK_{s+1}^T\\
&+\vec{\mu}_{s+1}\sum_{i=1}^{n}b_iK_{s+1}\Psi_iD_{s+1}V_{s+1}D_{s+1}^T\Psi_iK_{s+1}^T. \qquad (38)
\end{aligned}
$$

Under the assumption $P_{s|s}\le\bar{\mathcal{M}}_{s|s}$, by comparing (22) with (27), we arrive at $P_{s+1|s}\le\bar{\mathcal{M}}_{s+1|s}$ which, together with (23) and (38), further implies $P_{s+1|s+1}\le\bar{\mathcal{M}}_{s+1|s+1}$. The proof is now complete. ■

After deriving the upper bound $\bar{\mathcal{M}}_{s+1|s+1}$, the estimator gain is designed by minimizing $\bar{\mathcal{M}}_{s+1|s+1}$ at each time instant. The following theorem provides the estimator gain to minimize this upper bound.

Theorem 2: The upper bound $\bar{\mathcal{M}}_{s+1|s+1}$ of the EEC can be minimized by designing the estimator gain as follows:

$$
K_{s+1}=\mathcal{U}_{s+1}\mathcal{Y}_{s+1}^{-1} \qquad (39)
$$

where

$$
\begin{aligned}
\bar{\Psi}\triangleq&\mathrm{diag}\{b_1I,b_2I,\ldots,b_nI\},\\
\mathcal{U}_{s+1}\triangleq&(1+\beta_2)\vec{\mu}_{s+1}\bar{\mathcal{M}}_{s+1|s}C_{s+1}^T\bar{\Psi},\\
\mathcal{Y}_{s+1}\triangleq&(1+\beta_2)\sum_{i=1}^{n}b_i\vec{\mu}_{s+1}^2\Psi_iC_{s+1}\bar{\mathcal{M}}_{s+1|s}C_{s+1}^T\Psi_i\\
&+\Big(1+\tilde{\beta}\Big)\left(1+\beta_2^{-1}\right)\Big(\vec{\mu}_{s+1}-\vec{\mu}_{s+1}^2\Big)\\
&\times\sum_{i=1}^{n}b_i\Psi_iC_{s+1}\bar{\mathcal{M}}_{s+1|s}C_{s+1}^T\Psi_i\\
&+\Big(1+\tilde{\beta}^{-1}\Big)\left(1+\beta_2^{-1}\right)\Big(\vec{\mu}_{s+1}-\vec{\mu}_{s+1}^2\Big)\\
&\times\sum_{i=1}^{n}b_i\Psi_iC_{s+1}\hat{x}_{s+1|s}\hat{x}_{s+1|s}^TC_{s+1}^T\Psi_i\\
&+\sum_{i=1}^{n}b_i\vec{\mu}_{s+1}\Psi_iD_{s+1}V_{s+1}D_{s+1}^T\Psi_i. \qquad (40)
\end{aligned}
$$

Proof: The trace of the $\bar{\mathcal{M}}_{s+1|s+1}$ is computed as follows:

$$
\begin{aligned}
&\mathrm{tr}\left\{\bar{\mathcal{M}}_{s+1|s+1}\right\}\\
=&(1+\beta_2)\mathrm{tr}\Big\{\sum_{i=1}^{n}b_i\left(I-K_{s+1}\vec{\mu}_{s+1}\Psi_iC_{s+1}\right)\bar{\mathcal{M}}_{s+1|s}\\
&\times\left(I-K_{s+1}\vec{\mu}_{s+1}\Psi_iC_{s+1}\right)^T\Big\}+\Big(1+\tilde{\beta}\Big)\left(1+\beta_2^{-1}\right)\\
&\times\Big(\vec{\mu}_{s+1}-\vec{\mu}_{s+1}^2\Big)\mathrm{tr}\Big\{\sum_{i=1}^{n}b_iK_{s+1}\Psi_iC_{s+1}\bar{\mathcal{M}}_{s+1|s}C_{s+1}^T\\
&\times\Psi_iK_{s+1}^T\Big\}+\Big(1+\tilde{\beta}^{-1}\Big)\left(1+\beta_2^{-1}\right)\Big(\vec{\mu}_{s+1}-\vec{\mu}_{s+1}^2\Big)\\
&\times\mathrm{tr}\Big\{\sum_{i=1}^{n}b_iK_{s+1}\Psi_iC_{s+1}\hat{x}_{s+1|s}\hat{x}_{s+1|s}^TC_{s+1}^T\Psi_iK_{s+1}^T\Big\}\\
&+\mathrm{tr}\Big\{\vec{\mu}_{s+1}\sum_{i=1}^{n}b_iK_{s+1}\Psi_iD_{s+1}V_{s+1}D_{s+1}^T\Psi_iK_{s+1}^T\Big\}. \qquad (41)
\end{aligned}
$$

Then, we take the partial derivative of $\mathrm{tr}\{\bar{\mathcal{M}}_{s+1|s+1}\}$ with respect to the variable K_{s+1} and have

$$
\begin{aligned}
&\frac{\partial\mathrm{tr}\left(\bar{\mathcal{M}}_{s+1|s+1}\right)}{\partial K_{s+1}}\\
=&-2(1+\beta_2)\sum_{i=1}^{n}b_i\vec{\mu}_{s+1}\bar{\mathcal{M}}_{s+1|s}C_{s+1}^T\Psi_i\\
&+2(1+\beta_2)\sum_{i=1}^{n}b_i\vec{\mu}_{s+1}^2K_{s+1}\Psi_iC_{s+1}\bar{\mathcal{M}}_{s+1|s}C_{s+1}^T\Psi_i\\
&+2\Big(1+\tilde{\beta}\Big)\left(1+\beta_2^{-1}\right)\Big(\vec{\mu}_{s+1}-\vec{\mu}_{s+1}^2\Big)\\
&\times\sum_{i=1}^{n}b_iK_{s+1}\Psi_iC_{s+1}\bar{\mathcal{M}}_{s+1}C_{s+1}^T\Psi_i\\
&+2\Big(1+\tilde{\beta}^{-1}\Big)\left(1+\beta_2^{-1}\right)\Big(\vec{\mu}_{s+1}-\vec{\mu}_{s+1}^2\Big)K_{s+1}\\
&\times\sum_{i=1}^{n}b_i\Psi_iC_{s+1}\hat{x}_{s+1|s}\hat{x}_{s+1|s}^TC_{s+1}^T\Psi_i\\
&+2\sum_{i=1}^{n}b_iK_{s+1}\vec{\mu}_{s+1}\Psi_iD_{s+1}V_{s+1}D_{s+1}^T\Psi_i. \qquad (42)
\end{aligned}
$$

The gain parameter K_{s+1} can be determined by letting

$$
\frac{\partial\mathrm{tr}(\bar{\mathcal{M}}_{s+1|s+1})}{\partial K_{s+1}}=0. \qquad (43)
$$

Then, we have

$$
K_{s+1}=(1+\beta_2)\vec{\mu}_{s+1}\bar{\mathcal{M}}_{s+1|s}C_{s+1}^T\bar{\Psi}\mathcal{Y}_{s+1}^{-1}
$$

which ends the proof. ■

This article has been accepted for publication in a future issue of this journal, but has not been fully edited. Content may change prior to final publication.
Citation information: DOI: 10.1109/TSMC.2025.3612590, IEEE Transactions on Systems, Man, and Cybernetics: Systems

Remark 4: In this paper, a recursive state estimator is developed for nonlinear CPSs under the constraints imposed by the RAP-based token bucket strategy. To quantify the performance of the proposed estimator, an upper bound for the estimation error covariance is derived by formulating two Riccati-like difference equations. These equations systematically incorporate the impact of the RAP-based token bucket strategy on estimation. The proposed state estimation method effectively addresses practical challenges, such as limited transmission resources, making it highly applicable to real-world CPS scenarios. In the next section, numerical simulations will be conducted to validate the proposed method. Specifically, two key findings will be demonstrated: i) increasing the token generation rate improves estimation performance, and ii) reducing the token consumption rate enhances estimation accuracy. These findings will highlight the effectiveness of the proposed state estimation approach under constrained conditions.

Remark 5: The key contributions of this paper are summarized as follows.

1) A unified framework is presented to address the challenges posed by the RAP-based token bucket strategy in CPSs. This framework lays the groundwork for state estimation under practical resource constraints.
2) The model captures the stochastic nature of RAP scheduling and token consumption, offering a more realistic representation of CPS data transmission. By incorporating these uncertainties, the approach reflects real-world communication limitations.
3) The estimation error covariance bounds are derived using a set of coupled Riccati-like equations, balancing computational efficiency with analytical rigor.
4) The impact of key system parameters, such as token generation and consumption rates, is analyzed in detail, and this provides valuable insights into how communication constraints influence estimation performance.

These contributions enhance state estimation techniques for CPSs operating under network constraints, bridging theoretical development with practical application.

IV. An Illustrative Example

Consider a nonlinear CPS with the following system parameters:

$$A_s = \begin{bmatrix} 0.077 & 0.049+0.06\cos(s) & 0.060 & 0.048 & 0.067 \\ 0.390 & 0.050 & 0.072 & 0.085 & 0.085 \\ 0.079 & 0.040 & 0.082 & 0.074 & 0.055 \\ 0.085 & 0.045 & 0.078 & 0.045 & 0.089 \\ 0.095 & 0.084 & 0.058 & 0.026 & 0.060 \end{bmatrix},$$

$$C_s = \begin{bmatrix} 0.498 & 0.8+0.01\sin(s) & 0.699 & 0.456 & 0.254 \\ 0.512 & 0.120 & 0.723 & 0.254 & 0.265 \\ 0.980 & 0.872 & 0.458 & 0.254 & 0.848 \\ 0.480 & 0.620 & 0.865 & 0.257 & 0.978 \\ 0.860 & 0.212 & 0.421 & 0.254 & 0.578 \end{bmatrix},$$

$$B_s = \begin{bmatrix} 0.456 \\ 0.790+0.050\sin(s) \\ 0.699 \\ 0.895 \\ 0.052 \end{bmatrix}, D_s = \begin{bmatrix} 0.315+0.01\cos(s) \\ 0.565 \\ 0.245 \\ 0.615 \\ 0.550 \end{bmatrix}.$$

The nonlinear function is chosen as follows:

$$f(x_s) = \begin{bmatrix} 0.17\sin(x_{1,s}) \\ 0.16\sin(x_{2,s}) \\ 0.16\sin(x_{3,s}) \\ 0.17\sin(x_{4,s}) \\ 0.17\sin(x_{5,s}) \end{bmatrix}.$$

TABLE I
THE VALUE OF R_i AND THE PROBABILITY OF ITS BEING SELECTED b_i UNDER $\varepsilon = 3$

i	1	2	3	4	5
R_i	2	1	3	2	1
b_i	0.1051	0.2691	0.5182	0.1012	0.0064

TABLE II
THE VALUE OF R_i AND THE PROBABILITY OF ITS BEING SELECTED b_i UNDER $\varepsilon = 3$

i	1	2	3	4	5
R_i	3	4	4	2	3
b_i	0.2554	0.1322	0.0998	0.4432	0.0693

TABLE III
THE VALUE OF R_i AND THE PROBABILITY OF ITS BEING SELECTED b_i UNDER $\varepsilon = 3$

i	1	2	3	4	5
R_i	3	4	4	3	5
b_i	0.1505	0.4084	0.0559	0.0349	0.3503

The initial state is chosen as $x_s = \begin{bmatrix} 0.10 & 0.05 & 0.01 & 0.03 & 0.01 \end{bmatrix}^T$. The covariances of the measurement noise and process noise are selected as $V_s = 0.25$ and $W_s = 0.25$, respectively. Assume $S = 5$ (indicating a maximum token storage capacity of 5 units) and $z_0 = 1$ (indicating an initial token storage of 1 unit). The simulation results are shown in Figs. 1–14 and Tables I–III.

Based on Theorems 1–2, the minimum upper bound and the desired estimator gain can be calculated. To demonstrate how various parameters affect estimation performance, we give certain comparisons between different parameter values. Specifically, two scenarios with different token generation rates, $\varepsilon = 2$ and $\varepsilon = 3$, are examined. Additionally, three cases for different token consumption rates ψ_s are considered.

Tables I–III present the value of R_i corresponding to each node and the probability b_i that it is selected. Table I indicates that the bits assigned to $\vec{y}_{i,s}$ $(i = 1, 2, 3, 4, 5)$ are less than or equal to the token generation rate ($\varepsilon = 3$), i.e. $R_i \leq \varepsilon$. Table II indicates that the bits assigned to $\vec{y}_{i,s}$ $(i = 1, 2, 3, 4, 5)$ are either less than or equal to or greater than the token generation rate $\varepsilon = 3$, i.e. either $R_i < \varepsilon$ or $R_i = \varepsilon$ or $R_i > \varepsilon$. Table III indicates that the bits assigned to $\vec{y}_{i,s}$ $(i = 1, 2, 3, 4, 5)$ are greater than or equal to the token generation rate ($\varepsilon = 3$), i.e. $R_i \geq \varepsilon$.

This article has been accepted for publication in a future issue of this journal, but has not been fully edited. Content may change prior to final publication.
Citation information: DOI: 10.1109/TSMC.2025.3612590, IEEE Transactions on Systems, Man, and Cybernetics: Systems

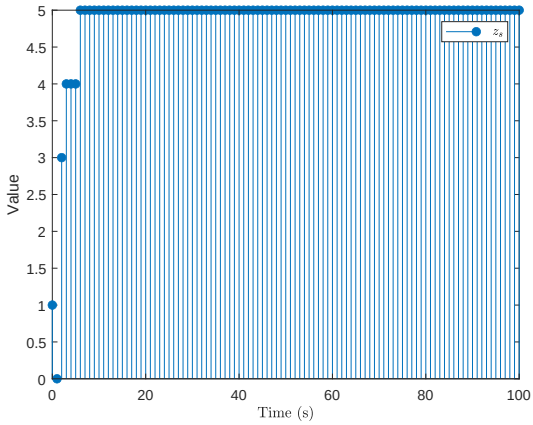

Fig. 1. The token bucket level at time s with $R_i \leq \varepsilon$.

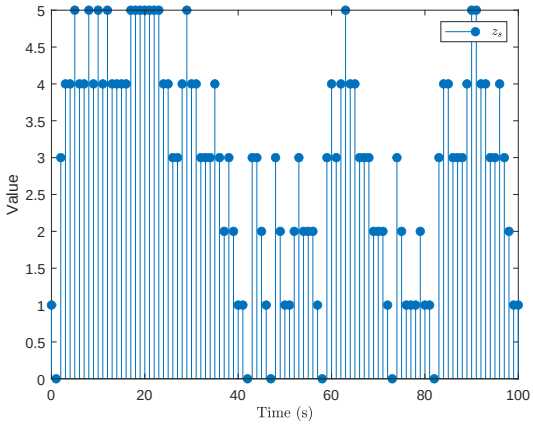

Fig. 4. The token bucket level with $R_i \leq \varepsilon$ or $R_i > \varepsilon$.

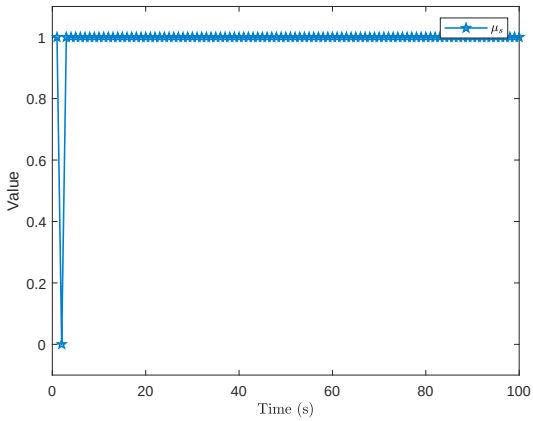

Fig. 2. The value of an indicator function with $R_i \leq \varepsilon$.

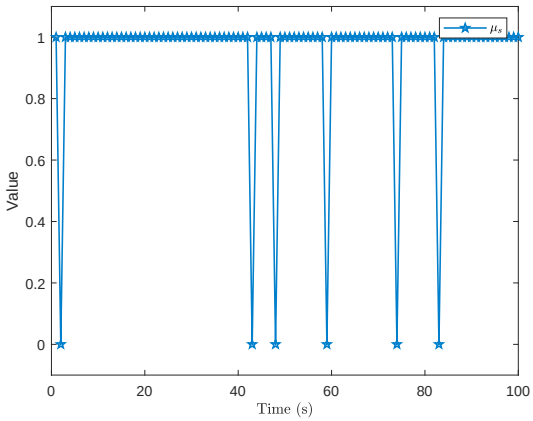

Fig. 5. The value of an indicator function with $R_i \leq \varepsilon$ or $R_i > \varepsilon$.

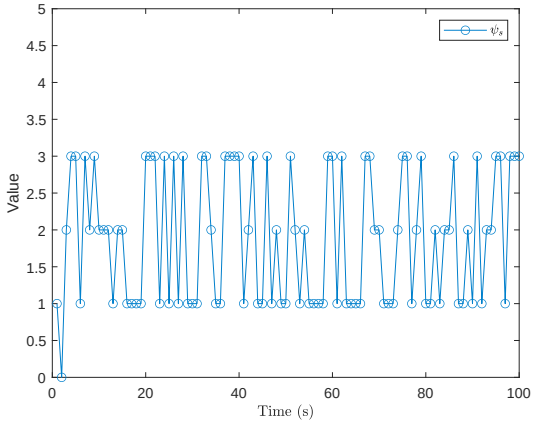

Fig. 3. The level of tokens consumed with $R_i \leq \varepsilon$.

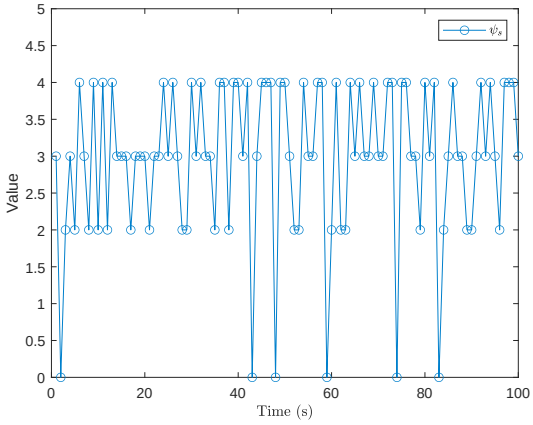

Fig. 6. The level of tokens consumed with $R_i \leq \varepsilon$ or $R_i > \varepsilon$.

Figs. 1–3, Figs. 4–6, and Figs. 7–9 indicate the token bucket level z_s, the number of tokens consumed ψ_s, and the success or failure of data transmission for the cases presented in Table I, Table II, and Table III, respectively. Specifically, Figs. 1, 4, and 7 display the amount of token stored in the bucket for different values of R_i. Figs. 2, 5, and 8 illustrate the value of the indicator function μ_s under varying R_i. Figs. 3, 6, and 9 show the level of token consumption for different values of R_i. From these results, it is evident that assigning fewer bits to the measurement signal leads to a lower token consumption rate. Furthermore, a higher number of tokens stored in the bucket increases the probability of successful data transmission (i.e.,

This article has been accepted for publication in a future issue of this journal, but has not been fully edited. Content may change prior to final publication.
Citation information: DOI: 10.1109/TSMC.2025.3612590, IEEE Transactions on Systems, Man, and Cybernetics: Systems

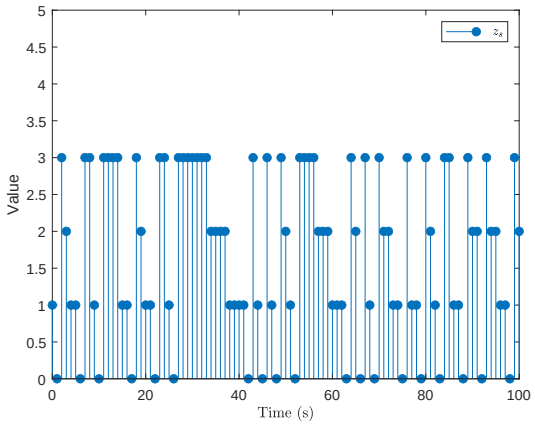

Fig. 7. The token bucket level with $R_i \geq \varepsilon$.

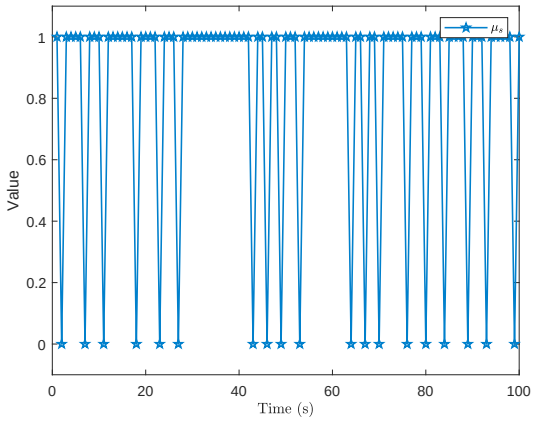

Fig. 8. The value of an indicator function with $R_i \geq \varepsilon$.

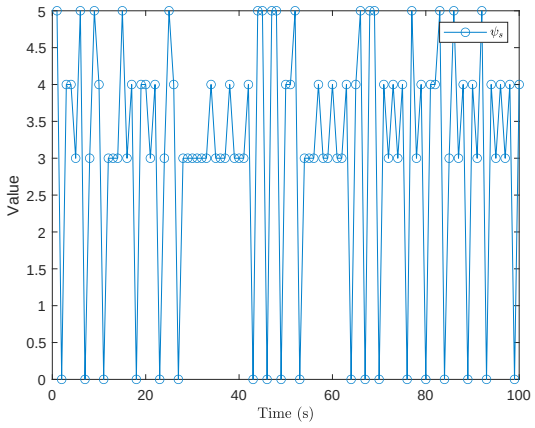

Fig. 9. The level of tokens consumed with $R_i \geq \varepsilon$.

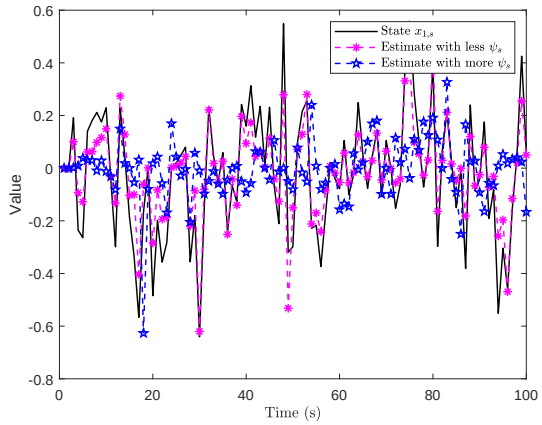

Fig. 10. The states and estimations with different ψ_s.

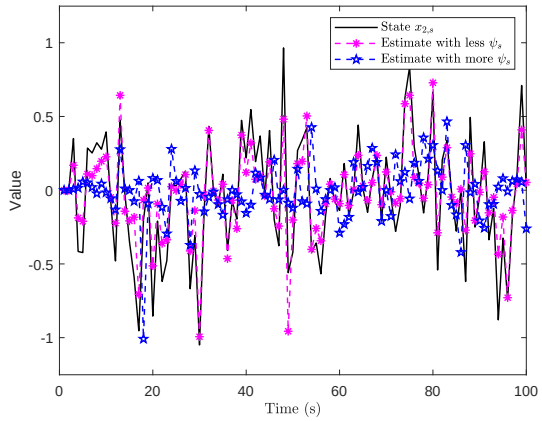

Fig. 11. The states and estimations with different ψ_s.

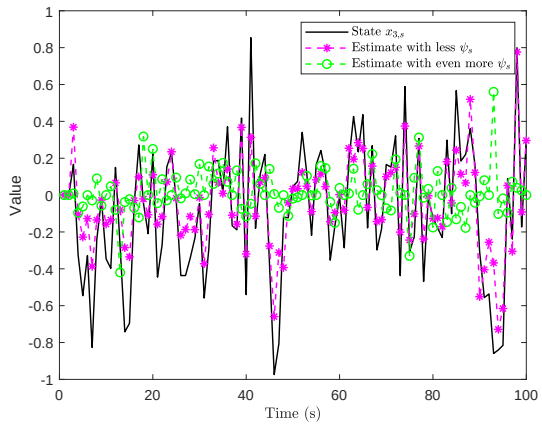

Fig. 12. The states and estimations with different ψ_s.

$\mu = 1$).

Figs. 10–13 illustrate the state trajectories of $x_{i,s}$ $(i = 1, 2, 3, 4)$ and their corresponding estimates $\hat{x}_{i,s}$ $(i = 1, 2, 3, 4)$ under varying ψ_s, which is influenced by different values of R_i. The results indicate that a higher ψ_s leads to a greater estimation error. This observation aligns with the expectation that an increased token consumption rate negatively impacts estimation accuracy.

Fig. 14 depicts the actual state $x_{5,s}$ and its estimate $\hat{x}_{5,s}$ under different token generation rates ε. As ε increases, the probability of successful transmission ($\mu_s = 1$) also rises, resulting in improved estimation performance. This trend reflects

This article has been accepted for publication in a future issue of this journal, but has not been fully edited. Content may change prior to final publication.
Citation information: DOI: 10.1109/TSMC.2025.3612590, IEEE Transactions on Systems, Man, and Cybernetics: Systems

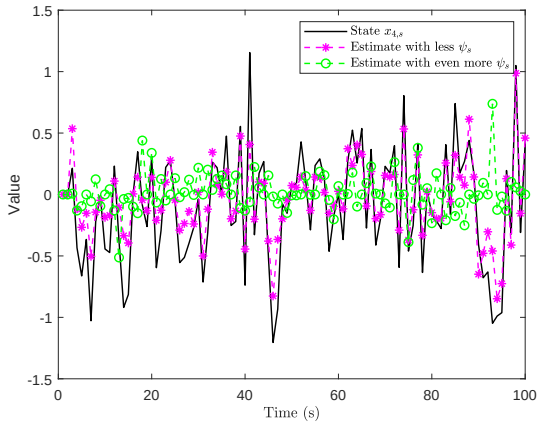

Fig. 13. The states and estimations with different ψ_s.

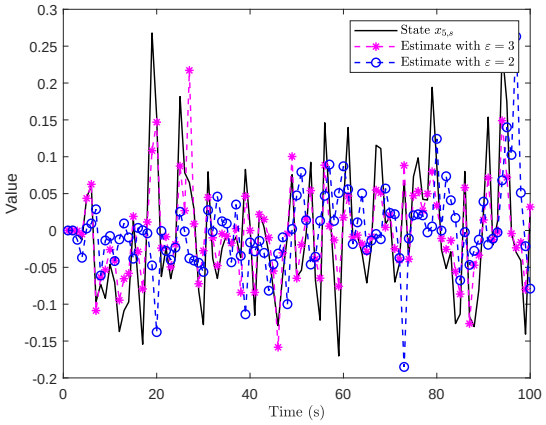

Fig. 14. The states and estimations with different ε.

the expected relationship between higher token generation rates and enhanced estimation accuracy.

In summary, all simulation results confirm the effectiveness of the proposed state estimation approach.

V. Conclusion

This paper has addressed the state estimation problem for CPSs, where measurement signals are transmitted over networks subject to the constraints imposed by the RAP-based token bucket strategy. The upper bound of the EEC has been rigorously derived using two coupled Riccati-like difference equations, establishing a solid theoretical foundation for the proposed method. Additionally, the optimal estimator gain has been obtained by minimizing this upper bound at each time step. To demonstrate the practical applicability of the proposed approach, a detailed example has been presented, illustrating its effectiveness in managing the challenges associated with the RAP-based token bucket strategy. The results confirm the method's capability to handle communication limitations while maintaining accurate state estimation, making it well-suited for real-world CPS applications operating under constrained resources. Looking ahead, several potential research directions can be explored: i) the proposed framework could be extended to incorporate other traffic management protocols such as the leaky bucket protocol; and ii) the current approach could be adapted to large-scale CPSs, which often involve complex network topologies with multiple interconnected components.

References

[1] A. I. Balan and V. T. Gopalakrishnan, Analysis of carrier sense multiple access protocols for channels supporting multi-packet reception, *IET Communications*, vol. 9, no. 4, pp. 468–475, Mar. 2015.

[2] P. B. Bithas, A. A. Rontogiannis and G. K. Karagiannidis, An improved threshold-based channel selection scheme for wireless communication systems, *IEEE Transactions on Wireless Communications*, vol. 15, no. 2, pp. 1531–1546, Feb. 2016.

[3] R. Caballero-Águila and J. Linares-Pérez, Centralized fusion estimation in networked systems: addressing deception attacks and packet dropouts with a zero-order hold approach, *International Journal of Network Dynamics and Intelligence*, vol. 3, no. 4, art. no. 100021, Dec. 2024.

[4] J. Cao, Z. Bu, Y. Wang, H. Yang, J. Jiang and H.-J. Li, Detecting prosumer-community group in smart grids from the multiagent perspective, *IEEE Transactions on Systems, Man, and Cybernetics: Systems*, vol. 49, no. 8, pp. 1652–1664, Aug. 2019.

[5] B. Chen, G. Hu, D. W. C. Ho and L. Yu, Distributed Kalman filtering for time-varying discrete sequential systems, *Automatica*, vol. 99, pp. 228–236, Jan. 2019.

[6] Y. Cui, Y. Liu, W. Zhang and F. E. Alsaadi, Sampled-based consensus for nonlinear multiagent systems with deception attacks: the decoupled method, *IEEE Transactions on Systems, Man, and Cybernetics: Systems*, vol. 51, no. 1, pp. 561–573, Jan. 2021.

[7] D. Ding, Q.-L. Han, Z. Wang and X. Ge, Recursive filtering of distributed cyber-physical systems with attack detection, *IEEE Transactions on Systems, Man, and Cybernetics: Systems*, vol. 51, no. 10, pp. 6466–6476, Oct. 2021.

[8] M. C. F. Donkers, W. P. M. H. Heemels, D. Bernardini, A. Bemporad and V. Shneer, Stability analysis of stochastic networked control systems, *Automatica*, vol. 48, no. 5, pp. 917–925, May 2012.

[9] A. Farraj, E. Hammad and D. Kundur, A cyber-physical control framework for transient stability in smart grids, *IEEE Transactions on Smart Grid*, vol. 9, no. 2, pp. 1205–1215, Mar. 2018.

[10] Z. Feng, W. Xu and J. Cao, Distributed Nash equilibrium computation under round-robin scheduling protocol, *IEEE Transactions on Automatic Control*, vol. 69, no. 1, pp. 339–346, Jan. 2024.

[11] M. J. García-Ligero, A. Hermoso-Carazo and J. Linares-Pérez, Distributed fusion estimation in network systems subject to random delays and deception attacks, *Mathematics*, vol. 10, no. 4, art. no. 662, Feb. 2022.

[12] H. Geng, Z. Wang, J. Hu, H. Dong and Y. Cheng, Distributed recursive filtering over sensor networks under random access protocol: when state saturation meets censored measurement, *IEEE Transactions on Cybernetics*, vol. 53, no. 12, pp. 7760–7772, Dec. 2023.

[13] F. Han, Z. Wang, H. Liu, H. Dong and G. Lu, Local design of distributed state estimators for linear discrete time-varying systems over binary sensor networks: a set-membership approach, *IEEE Transactions on Systems, Man, and Cybernetics: Systems*, vol. 54, no. 9, pp. 5641–5654, Sept. 2024.

[14] A. Hasan, I. Kuncara, A. Widyotriatmo, O. Osen and R. T. Bye, Secure state estimation and control for autonomous ships under cyberattacks, *Systems Science & Control Engineering*, vol. 13, no. 1, art. no. 2518964, 2025.

[15] M. Higgins, F. Teng and T. Parisini, Stealthy MTD against unsupervised learning-based blind FDI attacks in power systems, *IEEE Transactions on Information Forensics and Security*, vol. 16, pp. 1275–1287, Dec. 2021.

[16] Q. Hu, D. Fooladivanda, Y. H. Chang and C. J. Tomlin, Secure state estimation and control for cyber security of the nonlinear power systems, *IEEE Transactions on Control of Networks Systems*, vol. 5, no. 3, pp. 1310–1321, Sept. 2018.

[17] F. Jin, L. Ma, C. Zhao and Q. Liu, State estimation in networked control systems with a real-time transport protocol, *Systems Science & Control Engineering*, vol. 12, no. 1, art. no. 2347885, 2024.

[18] J. Kidambi, D. Ghosal and B. Mukherjee, Dynamic token bucket (DTB): a fair bandwidth allocation algorithm for high-speed networks, *Journal of High Speed Networks*, vol. 9, no. 2, pp. 67–87, Jan. 2000.

This article has been accepted for publication in a future issue of this journal, but has not been fully edited. Content may change prior to final publication.
Citation information: DOI: 10.1109/TSMC.2025.3612590, IEEE Transactions on Systems, Man, and Cybernetics: Systems

[19] C. Li, Y. Liu, M. Gao and L. Sheng, Fault-tolerant formation consensus control for time-varying multi-agent systems with stochastic communication protocol, *International Journal of Network Dynamics and Intelligence*, vol. 3, no. 1, art. no. 100004, Mar. 2024.

[20] Q. Li, Z. Wang, N. Li and W. Sheng, A dynamic event-triggered approach to recursive filtering for complex networks with switching topologies subject to random sensor failures, *IEEE Transactions on Neural Networks and Learning Systems*, vol. 31, no. 10, pp. 4381–4388, Oct. 2020.

[21] S. Linsenmayer and F. Allgówer, Performance oriented triggering mechanisms with guaranteed traffic characterization for linear discretetime systems, *2018 European Control Conference (ECC)*, pp. 1474–1479, Jun. 2018.

[22] J. Liu, E. Gong, L. Zha, X. Xie and E. Tian, Outlier-resistant recursive security filtering for multirate networked systems under fading measurements and round-robin protocol, *IEEE Transactions on Control of Network Systems*, vol. 10, no. 4, pp. 1962–1974, Dec. 2023.

[23] N. Liu and W. Qian, Stability analysis of low-voltage direct current system with time-varying delay, *Systems Science & Control Engineering*, vol. 12, no. 1, art. no. 2293918, Dec. 2024.

[24] X. Luo, H. Wu and Z. Li, NeuLFT: a novel approach to nonlinear canonical polyadic decomposition on high-dimensional incomplete tensors, *IEEE Transactions on Knowledge and Data Engineering*, vol. 35, no. 6, pp. 6148–6166, Jun. 2023.

[25] K. Mathews C. Kramer and R. Gotzhein, Token bucket based traffic shaping and monitoring for WLAN-based control systems, *2017 IEEE 28th Annual International Symposium on Personal, Indoor, and Mobile Radio Communications (PIMRC)*, pp. 1–7, Oct. 2017.

[26] X. Meng, H. Wang, Y. Li and Y. Shen, Unscented Kalman filtering for nonlinear systems with stochastic nonlinearities under FlexRay protocol, *International Journal of Network Dynamics and Intelligence*, vol. 4, no. 2, art. no. 100010, Jun. 2025.

[27] Z.-H. Pang, G.-P. Liu, D. Zhou and D. Sun, Data-based predictive control for networked nonlinear systems with network-induced delay and packet dropout, *IEEE Transactions on Industrial Electronics*, vol. 63, no. 2, pp. 1249–1257, Feb. 2016.

[28] Z.-H. Pang, L.-Z. Fan, Z. Dong, Q.-L. Han and G.-P. Liu, False data injection attacks against partial sensor measurements of networked control systems, *IEEE Transactions on Circuits and Systems II: Express Briefs*, vol. 69, no. 1, pp. 149–153, Jan. 2022.

[29] G. Procissi, A. Garg and M. Sanadidi, Token bucket characterization of long-range dependent traffic, *Computer Communications*, vol. 25, no. 11/12, pp. 1009–1017, Jul. 2002.

[30] W. Qian, D. Lu, S. Guo and Y. Zhao, Distributed state estimation for mixed delays system over sensor networks with multichannel random attacks and Markov switching topology, *IEEE Transactions on Neural Networks and Learning Systems*, vol. 35, no. 6, pp. 8623–8637, Jun. 2024.

[31] B. Qu, Z. Wang, B. Shen, H. Dong and H. Liu, Anomaly-resistant decentralized state estimation under minimum error entropy with fiducial points for wide-area power systems, *IEEE/CAA Journal of Automatica Sinica*, vol. 11, no. 1, pp. 74–87, Jan. 2024.

[32] Z. Sun and C. Han, Linear state estimation for multi-rate NCSs with multi-channel observation delays and unknown Markov packet losses, *International Journal of Network Dynamics and Intelligence*, vol. 4, no. 1, art. no. 100005, Mar. 2025.

[33] M. Tabbara and D. Nešić, Input-output stability of networked control systems with stochastic protocols and channels, *IEEE Transactions on Automatic Control*, vol. 53, no. 5, pp. 1160–1175, Jun. 2008.

[34] Y. Toroshanko, Y. Selepyna. N. Yakymchuk and V. Cherevyk, Control of traffic streams with the multi-rate token bucket, *2019 3rd International Conference on Advanced Information and Communications Technologies (AICT)*, pp. 352–355, Jul. 2019.

[35] V. Ugrinovskii and E. Fridman, A round-robin type protocol for distributed estimation with H_∞ consensus, *System and Control Letters*, vol. 69, pp. 103–110, Jul. 2014.

[36] F. Wang, J. Liang, J. Lam, J. Yang and C. Zhao, Robust filtering for 2-D systems with uncertain-variance noises and weighted try-once-discard protocols, *IEEE Transactions on Systems, Man, and Cybernetics: Systems*, vol. 53, no. 5, pp. 2914–2924, May 2023.

[37] J. Wang, J. Liang, K. Wang and Q. Li, Nonfragile output-feedback control for switched singular positive systems with time-varying delay under the round-robin protocol, *ISA Transactions*, vol. 146, pp. 142–153, Mar. 2024.

[38] W. Wang, X. Kan, D. Ding, H. Liu and X. Gao, Distributed correntropy Kalman filtering over sensor networks with FlexRay-based protocols, *International Journal of Systems Science*, vol. 56, no. 6, pp. 1347–1359, 2025.

[39] Y. Wang, Z. Wang, L. Zou and H. Dong, Observer-based fuzzy PID tracking control under try-once-discard communication protocol: an affine fuzzy model approach, *IEEE Transactions on Fuzzy Systems*, vol. 32, no. 4, pp. 2352–2365, Apr. 2024.

[40] S. Wildhagen, M. A. Müller and F. Allówer, Predictive control over a dynamical token bucket network, *IEEE Control Systems Letters*, vol. 3, no. 4, pp. 859–864, Oct. 2019.

[41] Y. Wu, Y. Niu and Y. Yang, Security sliding mode control for T-S fuzzy systems under attack probability-dependent dynamic round-robin protocol, *International Journal of Systems Science*, vol. 55, no. 5, pp. 926–940, Apr. 2024.

[42] L. Yang, Y. Xu, W. Lv, J.-Y. Li and L. Shi, Optimal transmission scheduling over multi-hop networks: structural results and reinforcement learning, *IEEE Transactions on Automatic Control*, vol. 69, no. 3, pp. 1826–1833, Mar. 2024.

[43] D. Yue, C. Deng, C. Wen and W. Wang, Finite-time distributed resilient tracking control for nonlinear MASs with application to power systems, *IEEE Transactions on Automatic Control*, vol. 69, no. 5, pp. 3128–3143, May 2024.

[44] R. Zhang, H. Liu, Y. Liu and H. Tan, Dynamic event-triggered state estimation for discrete-time delayed switched neural networks with constrained bit rate, *Systems Science & Control Engineering*, vol. 12, no. 1, art. no. 2334304, 2024.

[45] W. Zhang, Y. Zhao, H. Wang and Z. Yang, Robust model predictive control for polyhedral uncertain systems under relay and redundancy protocol, *International Journal of Systems Science*, vol. 56, no. 8, pp. 1617–1632, 2025.

[46] X.-M. Zhang, Q.-L. Han, X. Ge, D. Ding, L. Ding, D. Yue and C. Peng, Networked control systems: a survey of trends and techniques, *IEEE/CAA Journal of Automatica Sinica*, vol. 7, no. 1, pp. 1–17, Jan. 2019.

[47] Y. Zhang, D. Yue and E. Tian, Robust delay-distribution-dependent stability of discrete-time stochastic neural networks with time-varying delay, *Neurocomputing*, vol. 72, no. 4-6, pp. 1265–1273, Jan. 2009.

[48] L. Zou, Z. Wang, Q.-L. Han and D. H. Zhou, Recursive filtering for time-varying systems with random access protocol, *IEEE Transactions on Automatic Control*, vol. 64, no. 2, pp. 720–727, Feb. 2019.

Yu-Ang Wang received the B.Eng. degree in automation from the Shandong University of Science and Technology, Qingdao, Shandong, China, in 2020. She is currently pursuing the Ph.D. degree in Control Science and Engineering from Donghua University, Shanghai, China. From February 2023 to January 2025, she was a Visiting Ph.D. Student with the Department of Computer Science, Brunel University London, Uxbridge, U.K. From June 2025 to September 2025, she was a Research Assistant with the Department of Mechanical Engineering, The University of Hong Kong, Hong Kong.

Her current research interests include the control and filtering of networked system, cyber-attacks, watermarking, attack detection, token bucket protocol, and state estimation with energy harvesting constraints.

Miss Wang is a very active reviewer for many international journals.

This article has been accepted for publication in a future issue of this journal, but has not been fully edited. Content may change prior to final publication.
Citation information: DOI: 10.1109/TSMC.2025.3612590, IEEE Transactions on Systems, Man, and Cybernetics: Systems

Zidong Wang (SM'03-F'14) received the B.Sc. degree in mathematics in 1986 from Suzhou University, Suzhou, China, and the M.Sc. degree in applied mathematics in 1990 and the Ph.D. degree in electrical engineering in 1994, both from Nanjing University of Science and Technology, Nanjing, China.

He is currently a Professor of Dynamical Systems and Computing in the Department of Computer Science, Brunel University London, Uxbridge, U.K. From 1990 to 2002, he held teaching and research appointments in universities in China, Germany and the U.K. Prof. Wang's research interests include dynamical systems, signal processing, bioinformatics, control theory and applications. He has published a number of papers in international journals. He is a holder of the Alexander von Humboldt Research Fellowship of Germany, the JSPS Research Fellowship of Japan, William Mong Visiting Research Fellowship of Hong Kong.

Prof. Wang serves (or has served) as the Editor-in-Chief for *International Journal of Systems Science*, the Editor-in-Chief for *Neurocomputing*, the Editor-in-Chief for *Systems Science & Control Engineering*, and an Associate Editor for 12 international journals including IEEE Transactions on Automatic Control, IEEE Transactions on Control Systems Technology, IEEE Transactions on Neural Networks, IEEE Transactions on Signal Processing, and IEEE Transactions on Systems, Man, and Cybernetics-Part C. He is a Member of the Academia Europaea, a Member of the European Academy of Sciences and Arts, an Academician of the International Academy for Systems and Cybernetic Sciences, a Fellow of the IEEE, a Fellow of the Royal Statistical Society and a member of program committee for many international conferences.

Lei Zou received the Ph.D. degree in control science and engineering in 2016 from Harbin Institute of Technology, Harbin, China.

He is currently a Professor with the College of Information Science and Technology, Donghua University, Shanghai, China. From October 2013 to October 2015, he was a Visiting Ph.D. Student with the Department of Computer Science, Brunel University London, Uxbridge, U.K. His research interests include control and filtering of networked systems, moving-horizon estimation, state estimation subject to outliers, and secure state estimation.

Prof. Zou serves (or has served) as an Associate Editor for *Neurocomputing*, *International Journal of Systems Science*, *IEEE/CAA Journal of Automatica Sinica*, *IET Control Theory & Applications*, and *International Journal of Control, Automation and Systems*. He is a Senior Member of *IEEE* and *Chinese Association of Automation*, a Regular Reviewer of *Mathematical Reviews*, and a very active reviewer for many international journals.

Fan Wang received the Ph.D. degree in applied mathematics from Southeast University, Nanjing, China, in 2018.

She is currently a Professor with the School of Automation, Nanjing University of Information Science and Technology, Nanjing, China. From 2016 to 2018, she was a Visiting Ph.D. Student with the Department of Computer Science, Brunel University London, Uxbridge, U.K. From 2020 to 2021, she was a Post-Doctoral Fellow with the Department of Electrical and Computer Engineering, University of Macau, Macau, China. From 2022 to 2024, She was a Humboldt Research Fellow with the University of Duisburg-Essen, Duisburg, Germany. Her research interests include 2-D systems, networked control systems, recursive filtering, and optimal control.

Dr. Wang is a very active Reviewer for many international journals.

Hongli Dong received the Ph.D. degree in control science and engineering from the Harbin Institute of Technology, Harbin, China, in 2012.

From 2009 to 2010, she was a Research Assistant with the Department of Applied Mathematics, City University of Hong Kong, Hong Kong. From 2010 to 2011, she was a Research Assistant with the Department of Mechanical Engineering, The University of Hong Kong, Hong Kong. From 2011 to 2012, she was a Visiting Scholar with the Department of Information Systems and Computing, Brunel University London, Uxbridge, U.K. From 2012 to 2014, she was an Alexander von Humboldt Research Fellow with the University of Duisburg–Essen, Duisburg, Germany. She is currently a Professor with the Artificial Intelligence Energy Research Institute, Northeast Petroleum University, Daqing, China. She is also the Director of the Heilongjiang Provincial Key Laboratory of Networking and Intelligent Control, Daqing, China. Her current research interests include robust control and networked control systems.

Prof. Dong is a very active reviewer for many international journals.